The false paradox of phylogenetic signal: repeated origins of fossoriality in Xenarthra

Henrique José Schipanski[1]*; Iago Vinicios Geller[2]

[1] Departamento de Zoologia, Universidade Federal do Paraná, Curitiba, PR 81531980, Brazil.
[2] Universidade Federal de Santa Catarina, Araranguá, SC 88906072, Brazil.

*Corresponding author: henrique.schipanski@gmail.com

ABSTRACT

Phylogenetic signal is often read as evolutionary conservatism, but the same pattern can arise from retention of the ancestral state and repeated origins of the derived state. We tested this in Xenarthra using phylogenetic comparative analyses, ancestral state reconstructions, climatic associations, and tests of correlated evolution with diet, across 24 extant and extinct taxa and 2002 posterior trees. Fossoriality showed strong marginal phylogenetic structure ($D = -0.85$), yet ancestral state reconstructions indicated that this pattern reflects retention of the ancestral non-fossorial state rather than conservation of fossoriality. Fossoriality evolved repeatedly within Mylodontoidea, consistent with parallel evolution associated with shared morphological predispositions and similar ecological contexts. Precipitation regimes were associated with fossoriality, but the association reversed after excluding the lowest values, rejecting a simple climatic preference and pointing instead to precipitation as a viability filter rather than a driver. We also found support for correlated evolution between fossoriality and animal-based diets, although the direction of this relationship remains unresolved. Our results show that strong phylogenetic signal can mask repeated origins of a derived state, and that specialized lifestyles are better explained by interactions among phylogenetic history, environmental filtering, and foraging opportunity than by any single driver.

Keywords: ancestral state reconstruction; correlated evolution; fossoriality; phylogenetic signal; precipitation; Xenarthra.

INTRODUCTION

The diversification of lifestyles is a central dimension of mammalian ecological evolution, reflecting different strategies for exploiting the environment. Occupying terrestrial and arboreal strata imposes distinct functional and ecological demands associated with locomotion, foraging, protection, and climatic exposure. Among these specializations, fossoriality (i.e., the habit of digging and/or living in underground structures) has evolved repeatedly and can provide protection against predators, access to resources, and buffering against surface climatic conditions (Dondas et al., 2009; Hopkins, 2005; Vleck, 1981; Milling et al., 2018). Its evolution, however, involves a distinction between morphological capacity and ecological viability. Anatomical specializations enable excavation, whereas environmental conditions determine where digging is feasible and what benefits can be gained from it.

The traditional climatic hypothesis proposes that underground environments provide refuge from thermal or hydric stress, linking fossoriality to arid or thermally extreme environments (McNab, 1966; Gamble et al., 2000; Hasiotis et al., 2004; Baldo et al., 2016). However, the conditions that make burrows beneficial are not necessarily those that facilitate excavation. Subsurface resources (e.g., roots, tubers, fungi, and invertebrates) may provide additional benefits, whereas soil properties impose mechanical and energetic constraints (Vleck, 1981; Vizcaíno et al., 2001; Doody et al., 2024). In excessively dry environments, reduced availability of subsurface resources or increased excavation costs may limit the exploitation of this stratum (Frank et al., 2012; Lopes et al., 2017). Thus, an association between fossoriality and precipitation may reflect not a direct climatic preference, but rather exclusion from environments where conditions are unsuitable (Pinkert et al., 2025).

Xenarthra provides a suitable system for investigating these relationships because it combines ecological and morphological diversity with an evolutionary history documented by both extant and fossil representatives (Gaudin & Croft, 2015). The group encompasses lineages with different lifestyles, ranging from predominantly arboreal to terrestrial forms, some of which exhibit specializations for excavation (Gaudin & Croft, 2015). The South American ichnofossil record highlights the importance of this strategy (Buchmann et al., 2009; Dondas et al., 2009). Large paleoburrows (tunnels) are primarily attributed to extinct giant ground sloths, documenting extensive underground construction during the Neogene and Quaternary (Buchmann et al., 2009, 2016; Dondas et al., 2009; Frank et al., 2011, 2013). Nevertheless, the function of these structures and the environmental conditions associated with the evolution of excavation remain uncertain (Lopes et al., 2017).

Beyond climate, resource exploitation may also have contributed to dietary diversification. Excavation provides access to food resources that are unavailable or less accessible at the surface, and dietary strategies involving animal matter, such as omnivory and specialized myrmecophagy, may be associated with this specialization (Vleck, 1981; Gaudin & Croft, 2015). Morphological traits, environmental conditions, and dietary strategies are often interdependent. The ability to exploit the subsurface may precede dietary shifts, whereas favorable environmental conditions may turn this capacity into new foraging opportunities. Correlated evolution between ecological traits can reveal such associations, although it cannot establish their causal or temporal direction. However, these associations may also reflect broader differences among lineages, including their lifestyles and morphological characteristics, and therefore do not necessarily indicate that fossoriality promoted dietary shifts.

Distinguishing among these processes requires explicit consideration of phylogeny. The distribution of ecological traits may exhibit strong phylogenetic structure because closely related species share morphological, environmental, and dietary attributes, making it difficult to distinguish evolutionary conservatism from recurrent ecological associations (Boratyński et al., 2017; Pinkert et al., 2025). Summary metrics such as Fritz and Purvis' D for binary traits and Pagel's λ and Blomberg's K for continuous traits quantify phylogenetic clustering, but cannot independently identify which states are conserved or determine the number, direction,

or timing of evolutionary transitions (Fritz & Purvis, 2010; Pagel, 1999; Blomberg et al., 2003). Ancestral state reconstructions and tests of correlated evolution complement these measures.

Here, we investigate the evolution of fossorial specializations in Xenarthra and their associations with environmental conditions and dietary strategies. First, we quantify the phylogenetic structure of fossoriality and climatic variables. Next, we assess whether excessively arid conditions constrain the occurrence of fossorial specializations, rather than representing a gradient that directly favors their evolution. Finally, we test for correlated evolution between fossoriality and dietary strategies and reconstruct ancestral states to investigate the evolutionary history of these transitions. We expected the distribution of fossoriality to reflect both evolutionary history and environmental constraints on underground exploitation, and its evolution to be associated with dietary strategies that expand foraging opportunities. Thus, we aim to understand how morphological predispositions, environmental conditions, and ecological opportunities have been associated with the evolution of fossoriality in Xenarthra.

METHODS

Occurrence data and climatic variables

We compiled occurrence data for 24 Xenarthra species, including extant and extinct taxa from Folivora, Vermilingua, and Cingulata. All fossil records were obtained exclusively from the Paleobiology Database (PaleoBioDB; https://paleobiodb.org; Varela et al., 2014). We extracted values for the 19 bioclimatic variables for the Last Glacial Maximum (LGM; approximately 21 ka) from the PaleoClim database (http://www.paleoclim.org), at a spatial resolution of 5 arc-minutes (Brown et al., 2018). For each taxon, environmental values were extracted at the corresponding occurrence localities and summarized using the median, resulting in one climatic value per species for each variable.

The LGM was selected as a common environmental reference for three reasons: (i) it represents one of the most abrupt climatic transitions of the Quaternary, providing a scenario of extreme environmental conditions (Clark et al., 2009); (ii) it corresponds to an interval with a relatively high abundance of dated Quaternary Xenarthra fossils, allowing greater consistency in comparisons among occurrence records (Cione et al., 2009); and (iii) it is one of the periods for which comprehensive and relatively well-established paleoclimatic reconstructions are available (MARGO Project Members, 2009; Kageyama et al., 2018; Tierney et al., 2020). The LGM was used as a standardized spatial environmental reference for comparing taxa, rather than as a representation of the climatic conditions experienced during the origin or evolution of fossoriality. Therefore, climatic values were not interpreted as direct evidence of the temporal context in which the trait originated, but as a common environmental characterization of occurrence localities.

Selection of climatic variables

To reduce collinearity among predictors without introducing selection bias associated with the realized niches of the species, we generated 10000 random points across the geographic extent represented by the climatic raster and calculated variance inflation factors (VIFs) for the 19 bioclimatic variables (Table S1). This procedure allowed us to assess collinearity across the available environmental space, independently of the taxa's occurrence distributions, thereby avoiding having the species composition of the sample determine predictor selection. Variables with VIF > 3 were removed from subsequent analyses (Zuur et al., 2009; Table S2).

Phenotypic trait coding

Fossoriality and diet were coded individually for each taxon based on morphological and paleobiological evidence available in the literature. We did not adopt generalizations based solely on higher taxonomic categories, such as families (Gaudin & Croft, 2015).

Fossoriality was coded as a binary trait: 0 = absence of fossorial adaptations, including ambulatory, graviportal, suspensory, and other non-digging forms; and 1 = presence of fossorial adaptations, including subterranean, digging, and/or burrowing forms. Diet was also coded as a binary trait: 0 = strict herbivory, with no consumption of animal matter; and 1 = diet including animal matter, encompassing generalist omnivory, insectivory, myrmecophagy, and termitophagy.

Phylogeny and phylogenetic uncertainty

We used the posterior sample of phylogenies published by Presslee et al. (2019), comprising two combined MCMC runs after removal of the burn-in period, with a monophyly constraint imposed on *Bradypus* and all included non-folivoran outgroups. Fossil taxa lacking molecular data but used to inform the fossilized birth-death prior were pruned from the trees, resulting in 24 Xenarthra terminals spanning Folivora, Vermilingua, and Cingulata (Presslee et al., 2019). We retained all 2002 posterior trees to propagate phylogenetic uncertainty throughout all comparative analyses, including estimates of phylogenetic signal, regressions, ancestral state reconstructions, and tests of correlated evolution.

Phylogenetic signal

We assessed the phylogenetic structure of climatic variables and fossoriality before investigating their associations. For continuous climatic variables, we calculated Pagel's λ (Pagel, 1999) and Blomberg's K (Blomberg et al., 2003) across each of the 2002 posterior phylogenies using the *phytools* package (Revell, 2012). Pagel's λ quantifies the extent to which the covariance structure among taxa corresponds to that expected from their phylogenetic relationships, whereas Blomberg's K compares the observed phylogenetic structure with the expectation under a Brownian motion model.

For fossoriality, coded as a binary trait, we calculated Fritz and Purvis' D statistic (Fritz & Purvis, 2010), implemented in the *phylo.d* function of the *caper* package (Orme et al., 2018). The D statistic evaluates the phylogenetic clustering of state 1 (presence of fossorial adaptations) relative to two expectations: a random distribution of states among terminals (D = 1) and a distribution expected under a threshold Brownian motion model (D = 0). Negative values indicate stronger clustering than expected under this model. Although it quantifies the phylogenetic structure of trait distribution, D cannot independently identify which lineages retained a particular state, nor the number, direction, or timing of evolutionary transitions. These questions were investigated through ancestral state reconstructions. Trees containing zero-length branches were corrected using *dispRity::remove.zero.brlen* (Guillerme, 2018) before the analyses.

Phylogenetic logistic regression

We tested the association between climatic variables and fossoriality while accounting for phylogenetic non-independence among taxa. To this end, we fitted phylogenetic logistic regressions using the *phyloglm* function from the *phylolm* package (Ho & Ané, 2014), with the logistic_MPLE method. Models were fitted independently to each of the 2002 posterior trees, using 1,000 bootstrap replicates per fit to estimate confidence intervals for the coefficients. Coefficients and their corresponding intervals were subsequently summarized across trees using medians and 95% intervals. We also extracted the residual phylogenetic parameter α from each model, which quantifies residual phylogenetic correlation after accounting for the climatic predictor. Lower α values indicate stronger residual phylogenetic dependence, whereas higher values indicate weaker correlation among residuals associated with shared evolutionary history. Models that failed due to boundary estimates or convergence problems were excluded from the corresponding summaries.

Additionally, we conducted a common-support analysis for precipitation of the warmest quarter (BIO18), restricting models to values equal to or greater than 89.5 mm, corresponding to the lowest BIO18 value among fossorial taxa. This restriction removed the low-precipitation range represented exclusively by non-fossorial taxa, allowing us to evaluate the association between precipitation and fossoriality within the portion of environmental space where both states were represented. The upper limit was not restricted, thereby retaining records of high precipitation, including the few non-fossorial taxa occurring under these conditions, whose influence on the estimated association was also of interest.

Ancestral state reconstruction

We reconstructed ancestral fossoriality states at selected nodes using the *Fossil* command in BayesTraits v4 (Meade & Pagel, 2023). This approach allows the state of a focal node to be constrained to either 0 or 1 and estimates the corresponding marginal likelihood through stepping-stone sampling (Xie et al., 2011). Nodes were selected based on the maximum clade credibility tree (MCCT) from Presslee et al. (2019), which was used exclusively to establish correspondence among homologous nodes across the different posterior topologies. Each node

was then evaluated separately under the *Fossil 0* and *Fossil 1* models across all 2002 posterior trees, thereby propagating phylogenetic uncertainty into the ancestral state reconstructions.

For each node, marginal likelihoods were estimated using 500 stones, with 50,000 iterations per stone. The log Bayes factor was calculated as:

$$\log BF = 2 \times (\log ML_{Fossil0} - \log ML_{Fossil1})$$

Positive values favor state 0, corresponding to the absence of fossorial adaptations, whereas negative values favor state 1. Evidence strength was interpreted according to Kass and Raftery (1995).

Correlated evolution between fossoriality and diet

We tested whether fossoriality and diet exhibited correlated evolutionary histories using the independent and dependent models implemented in BayesTraits v4 (Pagel & Meade, 2006; Meade & Pagel, 2023). The independent model estimates transition rates for the two traits without allowing the rate of change in one trait to depend on the state of the other. In contrast, the dependent model allows the transition rates of each trait to vary according to the state of the other, making it possible to test whether the evolution of one trait is associated with changes in the transition dynamics of the second.

Marginal likelihoods were estimated through stepping-stone sampling, using 500 stones with 50,000 iterations per stone. All other model settings followed the default values in BayesTraits v4. The log Bayes factor was calculated as:

$$\log BF = 2 \times (\log ML_{dependent} - \log ML_{independent})$$

Positive values indicate greater support for the dependent model, whereas negative values favor the independent model. Evidence strength was interpreted according to Kass and Raftery (1995).

Sensitivity analysis

Because some fossoriality state assignments were uncertain, we assessed the sensitivity of our results to alternative codings. Eight taxa were identified as ambiguous, generating 256 possible coding configurations (2^8). These configurations were used to assess the sensitivity of the D statistic and of the phylogenetic logistic regression coefficients to alternative fossoriality coding decisions. For both the D statistic and the phylogenetic logistic regression coefficients, each of the 256 configurations was evaluated across a random subset of 202 posterior trees (approximately 10% of the 2002 trees), selected with a fixed random seed (42). This subset was used to reduce computational demand while retaining variation across posterior topologies, and the same subset was used for all configurations. To reduce computational demand, the sensitivity analysis of the phylogenetic logistic regression was run

without bootstrap replicates, using point estimates of the coefficient and α for each tree; the main analysis used 1000 bootstrap replicates per fit to estimate confidence intervals for the original coding.

For the correlated evolution analysis, we additionally evaluated uncertainty in the coding of both traits. Combining alternative fossoriality and diet codings resulted in 8192 possible configurations. From this set, we randomly sampled 500 configurations and fitted the independent and dependent models using the same analytical procedure described above. Unsuccessful fits were excluded, and the distribution of the resulting log-BF values was used to assess the robustness of the inference to uncertainty in trait coding.

RESULTS

Retention of the ancestral state and repeated origins of fossoriality

Ancestral state reconstructions conducted across all 2002 posterior trees consistently favored the absence of fossorial adaptations as the ancestral state at all major xenarthran nodes examined. Median log-BF values favored the non-fossorial state at the root of Xenarthra (3.82), Cingulata (2.96), Pilosa (10.65), Megalocnidae (13.65), Megatherioidea (13.69), Mylodontoidea (10.48), and the crown group of Mylodontidae (7.75). The only node favoring the fossorial state was the terminal pair *Mylodon darwinii* + *Glossotherium robustum* (median log-BF = −2.99). Reconstructions also indicated independent origins of fossoriality within Mylodontoidea, associated with the lineages *Scelidotherium* + *Scelidodon*, *Lestodon*, *Paramylodon*, and *Mylodon* + *Glossotherium* (Figure 1).

Phylogenetic structure of fossoriality and precipitation regimes

Fossoriality exhibited strong marginal phylogenetic structure, with a median Fritz and Purvis' D of −0.85 across the 2002 posterior trees (95% interval = [−1.28, −0.44]; Figure 2). D was negative in 99.7% of trees, and Brownian motion was rejected in all trees. Across the 256 alternative coding configurations, each evaluated across 202 posterior trees, D remained below 1 in all configurations and was negative in 82% of configuration-level medians (median D across configurations = −0.279; 95% interval = [−0.886, 0.134]). Per-tree median D was negative across all 202 trees (median = −0.282; 95% interval = [−0.513, −0.021]). The original coding produced one of the most negative estimates (D = −0.844), near the lower bound of the distribution of configuration-level medians, whereas the global median across all configurations remained negative (−0.277). The magnitude, but not the sign, of D was therefore sensitive to coding decisions (Figure S1).

All climatic variables retained after VIF screening showed varying degrees of phylogenetic signal across the 2002 posterior trees. Precipitation of the warmest quarter (BIO18; Figure S2) showed the strongest signal (median λ = 1.00; 95% interval = [0.99, 1.00]), followed by precipitation seasonality (BIO15; Figure S2; median λ = 1.00; 95% interval = [0.84, 1.00]) and precipitation of the coldest quarter (BIO19; median λ = 0.99; 95% interval = [0.92, 1.00]).

Temperature seasonality (BIO4) showed an intermediate signal (median $\lambda = 0.83$; 95% interval = [0.00, 1.00]), whereas mean diurnal range (BIO2) and precipitation of the driest month (BIO14) showed little or no detectable phylogenetic signal (median $\lambda \approx 0$; 95% interval = [0.00, 0.00] and [0.00, 1.00], respectively). Blomberg's K estimates were 0.317 for BIO14 (95% interval = [0.092, 0.429]), 0.574 for BIO15 (95% interval = [0.211, 0.735]), 1.012 for BIO18 (95% interval = [0.674, 1.295]), 0.442 for BIO19 (95% interval = [0.171, 0.671]), 0.276 for BIO2 (95% interval = [0.071, 0.371]), and 0.320 for BIO4 (95% interval = [0.105, 0.505]).

Association between fossoriality and precipitation regimes

Phylogenetic logistic models were successfully fitted across 1,814 posterior trees. Precipitation of the warmest quarter showed a positive association with fossoriality across all successfully fitted trees (median coefficient = 0.95; 95% interval = [0.52, 1.18]; Figure 3A). Precipitation seasonality showed a negative association (median = −1.36; 95% interval = [−1.52, −0.63]). The remaining climatic variables showed no detectable association with fossoriality. The residual phylogenetic parameter α after including precipitation of the warmest quarter had a median of 0.046 (95% interval = [0.042, 0.051]). The coefficient for this variable showed a weak positive correlation with α across trees ($r = 0.26$; Figure 3B).

In the analysis restricted to precipitation of the warmest quarter values equal to or greater than 89.5 mm, the coefficient for this variable changed from positive to negative (median = −0.34; 95% interval = [−0.43, −0.02]; Figure 4B), contrasting with the positive association observed in the full sample (Figure 4A).

The sensitivity analysis indicated that the climatic association was robust to alternative trait codings. Across the 256 configurations, each evaluated across 202 posterior trees, the coefficient for precipitation of the warmest quarter was positive in 97.5% of configurations (median = 0.429; 95% interval = [0.000, 1.392]). The original coding yielded a coefficient of 0.943, at the 87.5th percentile of the distribution but within its 95% interval (empirical $p = 0.129$). The residual phylogenetic parameter α remained low across all configurations (median = 0.057; 95% interval = [0.022, 0.091]), and the original coding was not extreme (empirical $p = 0.582$; Figure S3).

Correlated evolution between fossoriality and diet

The dependent model of correlated evolution was favored over the independent model (log-BF = 2.39). Among the 500 alternative coding configurations sampled from the 8192 possible combinations, 500 yielded successful fits, of which 97.6% favored the dependent model (Figure S4). The observed Bayes factor corresponded to the 18th percentile of the distribution, and the median BF across configurations (3.96) was 1.66 times the observed value. The dependent model was favored (BF > 0) in 97.6% of configurations, with positive evidence (BF > 2) in 88.0% and strong evidence (BF > 6) in 32.6%.

DISCUSSION

The false paradox of phylogenetic signal

Fossoriality showed negative marginal phylogenetic structure, a pattern conventionally read as evolutionary conservatism. Ancestral state reconstructions, however, favored the non-fossorial state at all major xenarthran nodes examined, with fossoriality arising independently in several Mylodontoidea lineages. These results are not contradictory. D quantifies the phylogenetic clustering of a binary trait but cannot identify which state is ancestral or conserved, nor the number, direction, or timing of transitions (Fritz & Purvis, 2010). Here, the signal results from two coinciding patterns: widespread retention of the ancestral non-fossorial state and restriction of the derived state to Mylodontoidea. It therefore describes how the trait is distributed on the tree, not the conservation of fossoriality. Pagel's λ and Blomberg's K share this interpretative limitation (Pagel, 1999; Blomberg et al., 2003; Revell et al., 2008; Münkemüller et al., 2015), which is a warning against reading marginal patterns as mechanisms rather than a flaw of the statistics. Similar patterns may arise whenever a derived phenotype evolves repeatedly within a restricted portion of the phylogeny, particularly among lineages sharing ecological contexts (Hardy & Pavoine, 2012; Losos, 2011). Because precipitation of the warmest quarter and precipitation seasonality are themselves strongly structured, part of the clustering in fossoriality probably also tracks the retention of precipitation regimes across lineages. The magnitude of D was sensitive to trait coding, but its sign was not: D remained negative across all alternative configurations, so the direction of the signal is robust even though its magnitude should not be overinterpreted.

Phylogenetic concentration and its inferential consequences

All seven fossorial taxa belong to Mylodontoidea, whereas the 17 non-fossorial taxa are distributed among non-mylodontoid Folivora, Vermilingua, and Cingulata (Figure 1). Although reconstructions indicate independent origins, these occurred within a single clade whose lineages share part of their history, morphology, and ecological context. The effective number of independent observations for the fossorial state is therefore smaller than the number of taxa exhibiting it, and climatic and dietary associations cannot be fully separated from membership in Mylodontoidea. This restricts the scope of our inferences without invalidating them. The converse is equally informative: non-fossoriality persisted across lineages and under a wide range of precipitation regimes, so an equally important question is why non-fossoriality remained the predominant condition throughout xenarthran diversification. Our results address the conditions associated with the origin and distribution of fossoriality within Mylodontoidea; they do not claim to identify a general law of xenarthran evolution.

Precipitation regimes and fossoriality

The classical climatic hypothesis predicts that fossoriality is favored in arid or thermally extreme environments, where burrows buffer adverse surface conditions (McNab, 1966; Gamble et al., 2000; Hasiotis et al., 2004; Baldo et al., 2016). Our results support neither this

hypothesis nor a simple preference for wetter environments. Precipitation of the warmest quarter was positively associated with fossoriality in the full sample, but this slope was produced by non-fossorial taxa occupying a dry range (< 89.5 mm) where no fossorial taxon occurs. Within the range where both states co-occur, the association was flat to slightly negative (Figure 4B). Precipitation seasonality was negatively associated with fossoriality. The association is therefore non-monotonic: fossoriality is absent under the driest regimes but does not increase continuously with precipitation. This pattern is more consistent with a viability filter than with a direct climatic driver. The restricted model has limited power (N = 12, five non-fossorial taxa), and its cutoff is defined by the lowest fossorial value, so we treat the flat-to-negative slope as weakening, not rejecting, a monotonic effect. Because precipitation is phylogenetically structured, the empty dry portion of the gradient is also compatible with Mylodontoidea occupying wetter regions for reasons unrelated to excavation. Thermal buffering may still contribute, but thermoregulation alone does not explain the observed distribution.

Edaphic mechanism: a hypothesis to be tested

The combination of a positive association in the full sample, a flat-to-negative association within common support, and a negative association with seasonality points to an indirect pathway through substrate properties. Cohesion, bulk density, hardness, and penetration resistance vary with moisture and affect the energetic cost of excavation (Mouazen et al., 2002; Ebensperger & Bozinovic, 2000), and in seasonal tropical and subtropical environments precipitation of the warmest quarter may partly index seasonal soil moisture (Romañach et al., 2005; Zelová et al., 2011). This is consistent with the absence of fossorial specializations in megatheriids, nothrotheriids, and glyptodonts associated with arid environments (McDonald, 2005; Zurita et al., 2011), and with their concentration in Mylodontidae from humid or seasonally humid settings (Bargo et al., 2000; Pujos et al., 2017; de Oliveira & Santos, 2018). We measured no soil properties, and resource availability or clade geography offer equally compatible explanations, so this remains a hypothesis. It generates testable predictions: paleoburrow localities should concentrate on substrates of intermediate moisture and low penetration resistance, and fossorial taxa in drier areas should coincide with more friable soils.

The foraging hypothesis and the association with animal-based diets

The dependent model of correlated evolution was favored over the independent model, and of the 500 alternative coding configurations that fitted successfully, 97.6% favored the dependent model, so the association is robust to coding uncertainty. It is also asymmetric: the only non-fossorial species with an animal-based diet is the strictly arboreal myrmecophage *Cyclopes didactylus* (Best & Harada, 1985; Hayssen et al., 2012). Animal-based diets can thus occur without fossoriality, whereas fossoriality was uncommon among lineages lacking animal-based diets. The traits are associated but not mutually dependent. This supports the hypothesis that subsurface exploitation provides additional foraging opportunities (Gaudin & Croft, 2015), in line with evidence of animal matter in the diet of *Mylodon darwinii* (Tejada et al., 2021). The analysis does not establish causal or temporal direction: fossoriality may

facilitate access to animal resources, animal-based diets may favor digging, or both may covary with a third factor such as precipitation regime. Finer dietary resolution is needed to identify which resources are most closely associated with fossoriality.

Parallel evolution under shared conditions

Fossoriality did not originate at the base of Mylodontoidea but evolved independently in different lineages within it. This is consistent with parallel evolution among lineages sharing morphological and ecological backgrounds. Mylodontoids exhibit robust forelimbs, enlarged claws, and well-developed musculature (Bargo et al., 2000; de Oliveira & Santos, 2018; Patiño et al., 2021), which likely provided the capacity for excavation, whereas precipitation regimes and foraging opportunities conditioned its viability. These three dimensions—morphological predisposition, environmental constraint, and ecological opportunity—need not operate independently: morphology enables excavation but does not determine its adoption; environment delimits where it is viable without inducing it; and subsurface resources may favor its maintenance (Gaudin & Croft, 2015; Presslee et al., 2019; Sansalone et al., 2020; Serio et al., 2020; Pinkert et al., 2025). This integrated scenario explains repeated origins within Mylodontoidea without requiring inheritance from a deeply specialized ancestor.

Implications for phylogenetic comparative studies

A strongly negative D could be read as evidence of conservatism, yet fossoriality was not ancestral in Xenarthra or Mylodontoidea. Marginal measures of phylogenetic signal should therefore be treated as properties of trait distributions, not as evolutionary mechanisms. Combining ancestral state reconstructions, ecological covariates, and tests of trait association helps distinguish retention of ancestral states, repeated evolution of derived ones, and shared environmental context (Schultz et al., 1996; Cunningham et al., 1998; Freckleton et al., 2002; Revell, 2010). This distinction is particularly important when a binary trait is concentrated in a single clade and environmental variables are also phylogenetically structured.

Limitations

Climatic values come from an LGM surface projected onto localities of taxa of different ages, so they do not necessarily represent conditions contemporary with the fossils or with the origin of the traits; other periods could test whether the associations hold through time. The sample (N = 24) limits power, particularly in the logistic regressions and correlated evolution tests, and the concentration of fossorial taxa in Mylodontoidea limits the separation of fossoriality effects from clade membership. The fossil record is unevenly distributed across taxa, regions, and periods, so precipitation values may partly reflect preservation and sampling biases. Trait coding required interpretation for extinct taxa; although sensitivity analyses show the results do not depend on a single configuration, the diet category pools distinct strategies and a single median per species ignores variation among localities.

CONCLUSIONS

Fossoriality in Xenarthra is not a deeply conserved ancestral state but a specialization that evolved repeatedly within Mylodontoidea. Its strong phylogenetic signal is a false paradox: it reflects retention of non-fossoriality rather than conservation of excavation. Precipitation appears to act as a viability filter, potentially mediated by substrate mechanical properties, rather than as a direct driver of fossoriality evolution. The evolution of excavation depends on the interplay between morphological capacity and foraging opportunities. The evolutionary history of fossoriality in Xenarthra is therefore less about a specific climate and more about the interaction between predisposition, opportunity, and constraint.

CRediT

Henrique José Schipanski: Conceptualization (Lead); Data curation (Lead); Formal analysis (Lead); Funding acquisition (Lead); Investigation (Lead); Methodology (Lead); Project administration (Lead); Resources (Lead); Software (Lead); Validation (Lead); Visualization (Lead); Writing – original draft (Lead); Writing – review & editing (Equal). **Iago Vinicios Geller:** Conceptualization (Supporting); Writing – review & editing (Equal).

ACKNOWLEDGEMENTS

We thank Graham Slater, Ross MacPhee, and Samantha Presslee for their time and correspondence regarding the xenarthran phylogeny, and Graham Slater for kindly providing the posterior distribution of dated phylogenetic trees used in this study. We are also grateful to Marcos Soares Barbeitos for suggesting the use of the posterior distribution of phylogenetic trees, which expanded the original analyses beyond the maximum clade credibility tree, and for his advice on the use of stepping-stone sampling. Finally, we thank Matheus Salles for reading an earlier draft of the manuscript and providing valuable comments and suggestions.

FUNDING INFORMATION

HJS was funded by a PhD Scholarship from CNPq (140363/2023-8).

COMPETING INTERESTS STATEMENT

All authors declare no conflict of interest.

REFERENCES

Baldo, M. B., F. Luna, and C. D. Antenucci. 2016. Does acclimation to contrasting atmospheric humidities affect evaporative water loss in the South American subterranean rodent Ctenomys talarum? J. Mammal. 97:1312–1320. https://doi.org/10.1093/jmammal/gyw104

Bargo, M. S., S. F. Vizcaíno, F. M. Archuby, and R. E. Blanco. 2000. Limb bone proportions, strength and digging in some Lujanian (Late Pleistocene-Early Holocene) mylodontid ground

sloths (Mammalia, Xenarthra). J. Vertebr. Paleontol. 20:601–610. https://doi.org/10.1671/0272-4634(2000)020[0601:LBPSAD]2.0.CO;2

Best, R. C., and A. Y. Harada. 1985. Food habits of the silky anteater (Cyclopes didactylus) in the Central Amazon. J. Mammal. 66:780–781. https://doi.org/10.2307/1380807

Blomberg, S. P., T. Garland, and A. R. Ives. 2003. Testing for phylogenetic signal in comparative data: behavioral traits are more labile. Evolution 57:717–745. https://doi.org/10.1111/j.0014-3820.2003.tb00285.x

Boratyński, Z., J. C. Brito, J. C. Campos, J. L. Cunha, L. Granjon, T. Mappes, A. Ndiaye, B. Rzebik-Kowalska, and N. Serén. 2017. Repeated evolution of camouflage in speciose desert rodents. Sci. Rep. 7:3522. https://doi.org/10.1038/s41598-017-03444-y

Brown, J. L., D. J. Hill, A. M. Dolan, A. C. Carnaval, and A. M. Haywood. 2018. PaleoClim, high spatial resolution paleoclimate surfaces for global land areas. Sci. Data 5:180254. https://doi.org/10.1038/sdata.2018.254

Buchmann, F. S., R. P. Lopes, and F. Caron. 2009. Icnofósseis (paleotocas e crotovinas) atribuídos a mamíferos extintos no Sudeste e Sul do Brasil. Rev. Bras. Paleontol. 12:247–256. https://doi.org/10.4072/rbp.2009.3.07

Buchmann, F. S., H. T. Frank, V. M. S. Ferreira, and E. A. Cruz. 2016. Evidência de vida gregária em paleotocas atribuídas a Mylodontidae (preguiças-gigantes). Rev. Bras. Paleontol. 19:259–270. https://doi.org/10.4072/rbp.2016.2.09

Cione, A. L., E. P. Tonni, and L. Soibelzon. 2009. Did humans cause the Late Pleistocene-Early Holocene mammalian extinctions in South America in a context of shrinking open areas? In G. Haynes (ed.), American Megafaunal Extinctions at the End of the Pleistocene, pp. 125–144. Springer, Dordrecht. https://doi.org/10.1007/978-1-4020-8793-6_7

Clark, P. U., A. S. Dyke, J. D. Shakun, A. E. Carlson, J. Clark, B. Wohlfarth, J. X. Mitrovica, S. W. Hostetler, and A. M. McCabe. 2009. The Last Glacial Maximum. Science 325:710–714. https://doi.org/10.1126/science.1172873

Cunningham, C. W., K. E. Omland, and T. H. Oakley. 1998. Reconstructing ancestral character states: a critical reappraisal. Trends Ecol. Evol. 13:361–366. https://doi.org/10.1016/S0169-5347(98)01382-2

de Oliveira, A. M., and C. M. D. Santos. 2018. Functional morphology and paleoecology of Pilosa (Xenarthra, Mammalia) based on a two-dimensional geometric morphometrics study of the humerus. J. Morphol. 279:1455–1467. https://doi.org/10.1002/jmor.20882

Dondas, A., F. I. Isla, and J. L. Carballido. 2009. Paleocaves exhumed from the Miramar Formation (Ensenadan Stage-age, Pleistocene), Mar del Plata, Argentina. Quat. Int. 210:44–50. https://doi.org/10.1016/j.quaint.2009.07.001

Doody, J. S., S. Shukla, and S. T. Hasiotis. 2024. Why animals construct helical burrows: construction vs. post-construction benefits. Ecol. Evol. 14:e11181. https://doi.org/10.1002/ece3.11181

Ebensperger, L. A., and F. Bozinovic. 2000. Energetics and burrowing behaviour in the semifossorial degu Octodon degus (Rodentia: Octodontidae). J. Zool. 252:179–186. https://doi.org/10.1111/j.1469-7998.2000.tb00613.x

Frank, H. T., F. S. C. Buchmann, L. G. Lima, F. Caron, R. P. Lopes, and M. Fornari. 2011. Karstic features generated from large palaeovertebrates tunnels in southern Brazil. Espeleo-Tema 22:139–153

Frank, H. T., L. D. Oliveira, F. N. Vicroski, R. Breier, N. G. Pasqualon, T. Araújo, and F. Caron. 2012. The complex history of a sandstone-hosted cave in the state of Santa Catarina, Brazil. Espeleo-Tema 23:87–101

Frank, H. T., L. G. Lima, N. P. Gerhard, F. Caron, F. S. C. Buchmann, M. Fornari, and R. P. Lopes. 2013. Description and interpretation of Cenozoic vertebrate ichnofossils in Rio Grande do Sul State, Brazil. Rev. Bras. Paleontol. 16:83–96. https://doi.org/10.4072/rbp.2013.1.07

Freckleton, R. P., P. H. Harvey, and M. Pagel. 2002. Phylogenetic analysis and comparative data: a test and review of evidence. Am. Nat. 160:712–726. https://doi.org/10.1086/343873

Fritz, S. A., and A. Purvis. 2010. Selectivity in mammalian extinction risk and threat types: a new measure of phylogenetic signal strength in binary traits. Conserv. Biol. 24:1042–1051. https://doi.org/10.1111/j.1523-1739.2010.01455.x

Gamble, D. W., J. T. Dogwiler, and J. Mylroie. 2000. Field assessment of the microclimatology of tropical flank margin caves. Clim. Res. 16:37–50. https://doi.org/10.3354/cr016037

Gaudin, T. J., and D. A. Croft. 2015. Paleogene Xenarthra and the evolution of South American mammals. J. Mammal. 96:622–634. https://doi.org/10.1093/jmammal/gyv073

Guillerme, T. 2018. dispRity: a modular R package for measuring disparity. Methods Ecol. Evol. 9:1755–1763. https://doi.org/10.1111/2041-210X.13022

Hardy, O. J., and S. Pavoine. 2012. Assessing phylogenetic signal with measurement error: a comparison of Mantel tests, Blomberg et al.'s K, and phylogenetic distograms. Evolution 66:2614–2621. https://doi.org/10.1111/j.1558-5646.2012.01623.x

Hasiotis, S. T., R. W. Wellner, A. J. Martin, and T. M. Demko. 2004. Vertebrate burrows from Triassic and Jurassic continental deposits of North America and Antarctica: their paleoenvironmental and paleoecological significance. Ichnos 11:103–124. https://doi.org/10.1080/10420940490428760

Hayssen, V., F. Miranda, and B. Pasch. 2012. Cyclopes didactylus (Pilosa: Cyclopedidae). Mamm. Species 44:51–58. https://doi.org/10.1644/895.1

Ho, L. S. T., and C. Ané. 2014. A linear-time algorithm for Gaussian and non-Gaussian trait evolution models. Syst. Biol. 63:397–408. https://doi.org/10.1093/sysbio/syu005

Hopkins, S. S. B. 2005. The evolution of fossoriality and the adaptive role of horns in the Mylagaulidae (Mammalia: Rodentia). Proc. R. Soc. B 272:1705–1713. https://doi.org/10.1098/rspb.2005.3171

Kageyama, M., P. Braconnot, S. P. Harrison, A. M. Haywood, J. H. Jungclaus, B. L. Otto-Bliesner, J.-Y. Peterschmitt, A. Abe-Ouchi, S. Albani, P. J. Bartlein, C. Brierley, M. Crucifix, A. Dolan, L. Fernandez-Donado, H. Fischer, P. O. Hopcroft, R. F. Ivanovic, F. Lambert, D. J. Lunt, N. M. Mahowald, W. R. Peltier, S. J. Phipps, D. M. Roche, G. A. Schmidt, L. Tarasov, P. J. Valdes, Q. Zhang, and T. Zhou. 2018. The PMIP4 contribution to CMIP6 – Part 1: Overview and over-arching analysis plan. Geosci. Model Dev. 11:1033–1057. https://doi.org/10.5194/gmd-11-1033-2018

Kass, R. E., and A. E. Raftery. 1995. Bayes factors. J. Am. Stat. Assoc. 90:773–795. https://doi.org/10.1080/01621459.1995.10476572

Lopes, R. P., H. T. Frank, F. S. C. Buchmann, and F. Caron. 2017. Megaichnus igen. nov.: giant paleoburrows attributed to extinct Cenozoic mammals from South America. Ichnos 24:133–145. https://doi.org/10.1080/10420940.2016.1223654

Losos, J. B. 2011. Seeing the forest for the trees: the limitations of phylogenies in comparative biology. Am. Nat. 177:709–727. https://doi.org/10.1086/660020

MARGO Project Members. 2009. Constraints on the magnitude and patterns of ocean cooling at the Last Glacial Maximum. Nat. Geosci. 2:127–132. https://doi.org/10.1038/ngeo411

McDonald, H. G. 2005. Paleoecology of extinct xenarthrans and the Great American Biotic Interchange. Bull. Fla. Mus. Nat. Hist. 45:313–334. https://doi.org/10.58782/flmnh.zrar3244

McNab, B. K. 1966. The metabolism of fossorial rodents: a study of convergence. Ecology 47:712–733. https://doi.org/10.2307/1934259

Meade, A., and M. Pagel. 2023. BayesTraits V4.0.1. Manual. University of Reading, Reading.https://www.evolution.reading.ac.uk/BayesTraitsV4.0.0/Files/BayesTraitsV4.0.0-Manual.pdf

Milling, C. R., J. L. Rachlow, M. A. Chappell, M. J. Camp, T. R. Johnson, L. A. Shipley, D. R. Paul, and J. S. Forbey. 2018. Seasonal temperature acclimatization in a semi-fossorial mammal and the role of burrows as thermal refuges. PeerJ 6:e4511. https://doi.org/10.7717/peerj.4511

Mouazen, A. M., H. Ramon, and J. De Baerdemaeker. 2002. SW—Soil and Water: effects of bulk density and moisture content on selected mechanical properties of sandy loam soil. Biosyst. Eng. 83:217–224. https://doi.org/10.1006/bioe.2002.0103

Münkemüller, T., F. C. Boucher, W. Thuiller, and S. Lavergne. 2015. Phylogenetic niche conservatism – common pitfalls and ways forward. Funct. Ecol. 29:627–639. https://doi.org/10.1111/1365-2435.12388

Orme, D., R. Freckleton, G. Thomas, T. Petzoldt, S. Fritz, N. Isaac, and W. Pearse. 2018. caper: comparative analyses of phylogenetics and evolution in R. R package version 1.0.1. https://CRAN.R-project.org/package=caper

Pagel, M. 1999. Inferring the historical patterns of biological evolution. Nature 401:877–884. https://doi.org/10.1038/44766

Pagel, M., and A. Meade. 2006. Bayesian analysis of correlated evolution of discrete characters by reversible-jump Markov chain Monte Carlo. Am. Nat. 167:808–825. https://doi.org/10.1086/503444

Patiño, S., J. Pérez Zerpa, and R. A. Fariña. 2021. Finite element and morphological analysis in extant mammals' claws and Quaternary sloths' ungual phalanges. *Hist. Biol.* 33:857–867. https://doi.org/10.1080/08912963.2019.1664504

Pinkert, S., V. Reuber, L.-M. Krug, L. Heidrich, F. Rehling, R. Brandl, and N. Farwig. 2025. Burrowing facilitated the survival of mammals in harsh and fluctuating climates. Curr. Biol. 35:1779–1790.e3. https://doi.org/10.1016/j.cub.2025.02.064

Presslee, S., G. J. Slater, F. Pujos, A. M. Forasiepi, R. Fischer, K. Molloy, M. Mackie, J. V. Olsen, A. Kramarz, M. Taglioretti, F. Scaglia, M. Lezcano, J. L. Lanata, J. Southon, R. Feranec, J. Bloch, A. Hajduk, F. M. Martin, R. Salas Gismondi, M. Reguero, C. de Muizon, A. Greenwood, B. T. Chait, K. Penkman, and R. D. E. MacPhee. 2019. Palaeoproteomics resolves sloth relationships. Nat. Ecol. Evol. 3:1121–1130. https://doi.org/10.1038/s41559-019-0909-z

Pujos, F., G. De Iuliis, and C. Cartelle. 2017. A paleogeographic overview of tropical fossil sloths: towards an understanding of the origin of extant suspensory sloths? J. Mamm. Evol. 24:19–38. https://doi.org/10.1007/s10914-016-9330-4

Revell, L. J., L. J. Harmon, and D. C. Collar. 2008. Phylogenetic signal, evolutionary process, and rate. Syst. Biol. 57:591–601. https://doi.org/10.1080/10635150802302427

Revell, L. J. 2010. Phylogenetic signal and linear regression on species data. Methods Ecol. Evol. 1:319–329. https://doi.org/10.1111/j.2041-210X.2010.00044.x

Revell, L. J. 2012. phytools: an R package for phylogenetic comparative biology (and other things). Methods Ecol. Evol. 3:217–223. https://doi.org/10.1111/j.2041-210X.2011.00169.x

Romañach, S. S., O. J. Reichman, and E. W. Seabloom. 2005. Seasonal influences on burrowing activity of a subterranean rodent, Thomomys bottae. J. Zool. 266:319–325. https://doi.org/10.1017/S0952836905006941

Sansalone, G., S. Castiglione, P. Raia, M. Archer, B. Dickson, S. Hand, P. Piras, A. Profico, and S. Wroe. 2020. Decoupling functional and morphological convergence, the study case of fossorial Mammalia. Front. Earth Sci. 8:112. https://doi.org/10.3389/feart.2020.00112

Schultz, T. R., R. B. Cocroft, and G. A. Churchill. 1996. The reconstruction of ancestral character states. Evolution 50:504–511. https://doi.org/10.1111/j.1558-5646.1996.tb03863.x

Serio, C., P. Raia, and C. Meloro. 2020. Locomotory adaptations in 3D humerus geometry of Xenarthra: testing for convergence. Front. Ecol. Evol. 8:139. https://doi.org/10.3389/fevo.2020.00139

Tejada, J. V., J. J. Flynn, R. MacPhee, T. C. O'Connell, T. E. Cerling, L. Bermudez, C. Capuñay, N. Wallsgrove, and B. N. Popp. 2021. Isotope data from amino acids indicate Darwin's ground sloth was not an herbivore. Sci. Rep. 11:18944. https://doi.org/10.1038/s41598-021-97996-9

Tierney, J. E., J. Zhu, J. King, S. B. Malevich, G. J. Hakim, and C. J. Poulsen. 2020. Glacial cooling and climate sensitivity revisited. Nature 584:569–573. https://doi.org/10.1038/s41586-020-2617-x

Varela, S., González-Hernández, J., Sgarbi, L. F., Marshall, C., Uhen, M. D., Peters, S., & McClennen, M. 2014. paleobioDB: An R package for downloading, visualizing and processing data from the Paleobiology Database. Ecography, 37(12), 1246–1251. https://doi.org/10.1111/ecog.01154

Vizcaíno, S. F., M. Zárate, M. S. Bargo, and A. Dondas. 2001. Pleistocene burrows in the Mar del Plata area (Argentina) and their probable builders. Acta Palaeontol. Pol. 46:289–301.

Vleck, D. 1981. Burrow structure and foraging costs in the fossorial rodent, Thomomys bottae. Oecologia 49:391–396. https://doi.org/10.1007/BF00347605

Xie, W., P. O. Lewis, Y. Fan, L. Kuo, and M.-H. Chen. 2011. Improving marginal likelihood estimation for Bayesian phylogenetic model selection. Syst. Biol. 60:150–160. https://doi.org/10.1093/sysbio/syq085

Zelová, J., R. Šumbera, J. Okrouhlík, J. Šklíba, M. Lövy, and H. Burda. 2011. A seasonal difference of daily energy expenditure in a free-living subterranean rodent, the silvery mole-rat (Heliophobius argenteocinereus; Bathyergidae). Comp. Biochem. Physiol. A Mol. Integr. Physiol. 158:17–21. https://doi.org/10.1016/j.cbpa.2010.07.026

Zurita, A. E., A. C. Scarano, A. A. Carlini, G. J. Scillato-Yané, and E. Soibelzon. 2011. Neosclerocalyptus spp. (Cingulata: Glyptodontidae: Hoplophorini): cranial morphology and

palaeoenvironments along the changing Quaternary. J. Nat. Hist. 45:893–914. https://doi.org/10.1080/00222933.2010.536917

Zuur, A. F., E. N. Ieno, N. J. Walker, A. A. Saveliev, and G. M. Smith. 2009. Mixed effects models and extensions in ecology with R. Springer, New York. https://doi.org/10.1007/978-0-387-87458-6

Figures and table legends

Figure 1. Maximum clade credibility tree of 24 Xenarthran species, based on the posterior sample of 2002 trees from Presslee et al. (2019). Tip colors indicate fossorial state: blue = non-fossorial (0); red = fossorial (1). Branch lengths are proportional to time.

Figure 2. Distribution of Fritz & Purvis's D statistic across 2002 phylogenetic trees. The dashed red line marks D = 0 (Brownian motion); the dashed dark green line marks D = 1 (random phylogenetic structure); the solid black line marks the median (D = −0.85); dotted black lines mark the 95% interval across trees ([−1.28, −0.44]). Values of $D < 0$ indicate greater phylogenetic clustering than expected under Brownian motion; D = 0 is consistent with Brownian motion; D = 1 is consistent with random phylogenetic structure; $D > 1$ indicates greater dispersion than expected under random evolution. In 99.7% of trees, D was negative.

Figure 3. Results of phylogenetic logistic models across 1814 successfully fitted trees. (A) Histogram of the coefficient of precipitation of the warmest quarter (bio_18) across trees. The dashed red line marks zero; the solid black line marks the median (0.95); dotted black lines mark the 95% interval across trees ([0.52, 1.18]). The coefficient was positive in 100% of trees. **(B)** Relationship between the coefficient of bio_18 and the residual phylogenetic signal (α) across trees. Each point represents one tree. The red line shows the linear regression; r = 0.26.

Figure 4. Predictive curves of fossoriality probability as a function of precipitation of the warmest quarter (bio_18). Thin lines represent predictions from individual phylogenetic logistic models fitted; the shaded band represents the 95% interval of predictions across trees; the thick red line represents the median prediction. Points show observed data, with vertical jitter for visualization. **(A)** Full model (N = 24). The dotted vertical line marks the lower bound of the common climatic support (bio_18 = 89.5 mm), and the shaded rectangle indicates the range of bio_18 occupied by fossorial species. **(B)** Model restricted to the common climatic support (bio_18 ≥ 89.5; N = 12). The median curve is flat or slightly negative, indicating that the positive association observed in the full model was driven by non-fossorial species in very dry climates (bio_18 < 89.5), rather than by a positive preference for wetter climates among fossorial lineages.

Figure S1. Sensitivity of Fritz and Purvis' D to alternative fossoriality codings. Each of the 256 coding configurations for the eight ambiguous taxa was evaluated across a random subset of 202 posterior trees (approximately 10% of the 2002 trees). Points show median D per configuration; vertical bars show the 95% interval across trees. The original coding is highlighted. Configurations are ordered by median D. Per-tree median D (across configurations) was negative for all 202 trees (median = −0.282; 95% interval = [−0.513, −0.021]).

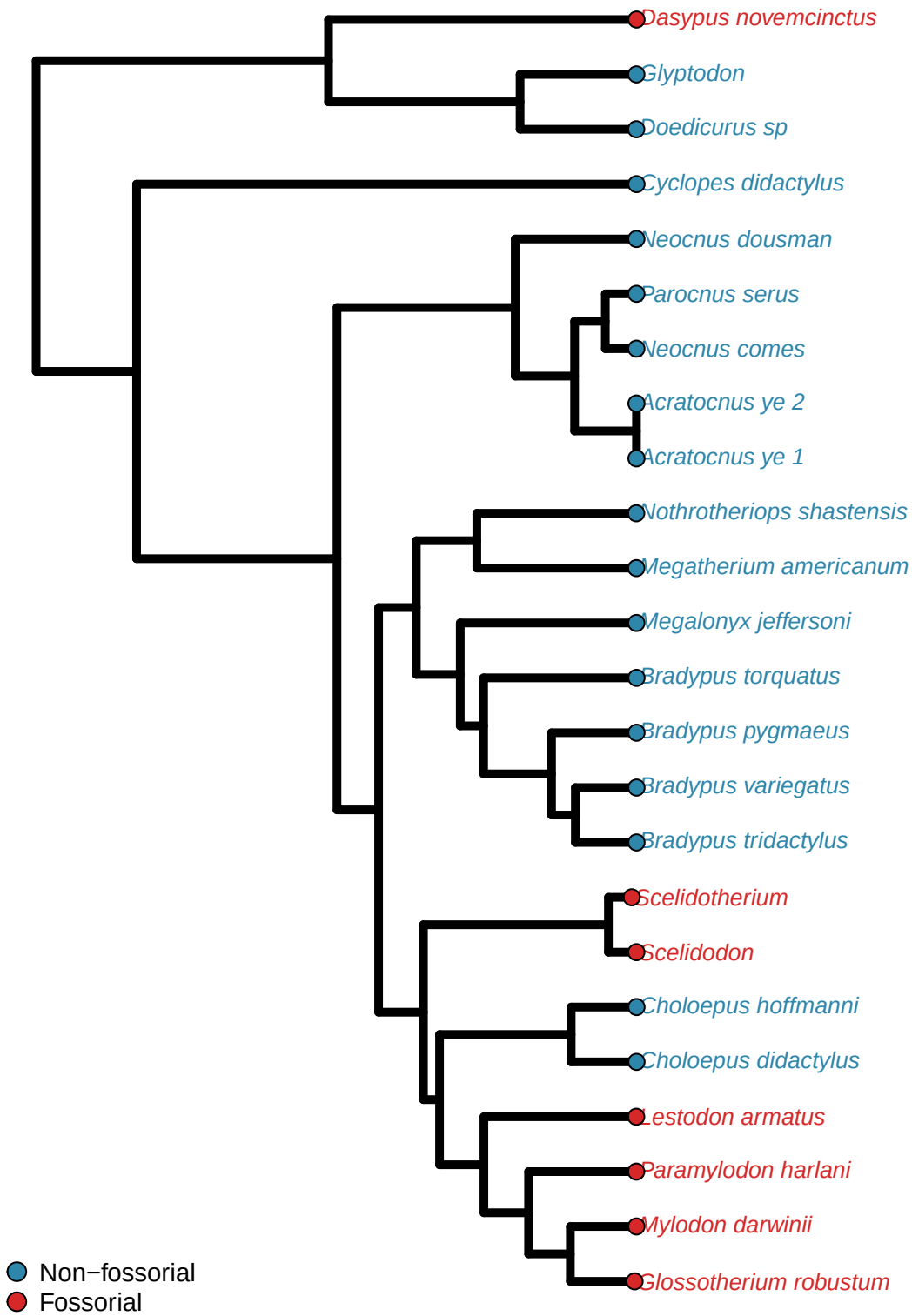
Figure S2. Distributions of phylogenetic signal metrics across 2002 posterior trees for six bioclimatic variables: mean diurnal range (bio_2), temperature seasonality (bio_4), precipitation of the driest month (bio_14), precipitation seasonality (bio_15), precipitation of the warmest quarter (bio_18), and precipitation of the coldest quarter (bio_19). For each variable, panels show Blomberg's K, associated P-values for K, Pagel's λ, and associated P-values for λ. Blomberg's K values were generally below 1, whereas Pagel's λ was close to 1 for bio_15, bio_18, and bio_19, indicating stronger phylogenetic dependence for precipitation-related variables.

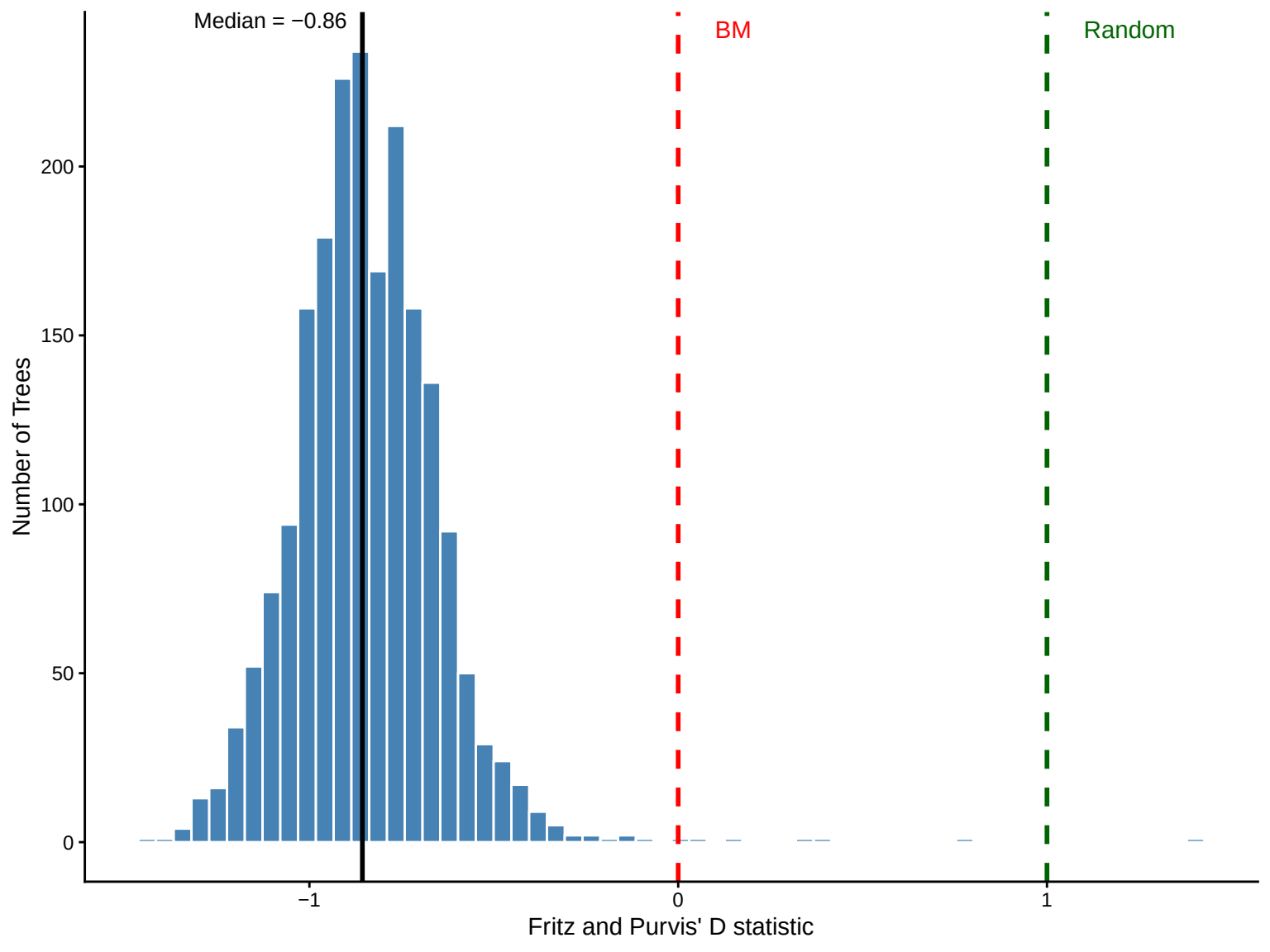
Figure S3. Sensitivity of the phylogenetic logistic regression to alternative trait codings. Distribution of the coefficient for precipitation of the warmest quarter (BIO18) across 256 coding configurations, each fitted across 202 posterior trees. The solid red line marks the coefficient for the original coding (0.943); the dashed grey line marks the mean of the distribution (0.429). The coefficient was positive in 97.5% of configurations, and the original coding fell within the 95% interval of the distribution (empirical p = 0.129). The residual phylogenetic parameter α remained low across all configurations (median = 0.057; 95% interval = [0.022, 0.091]), and the original coding was not extreme (empirical p = 0.582).

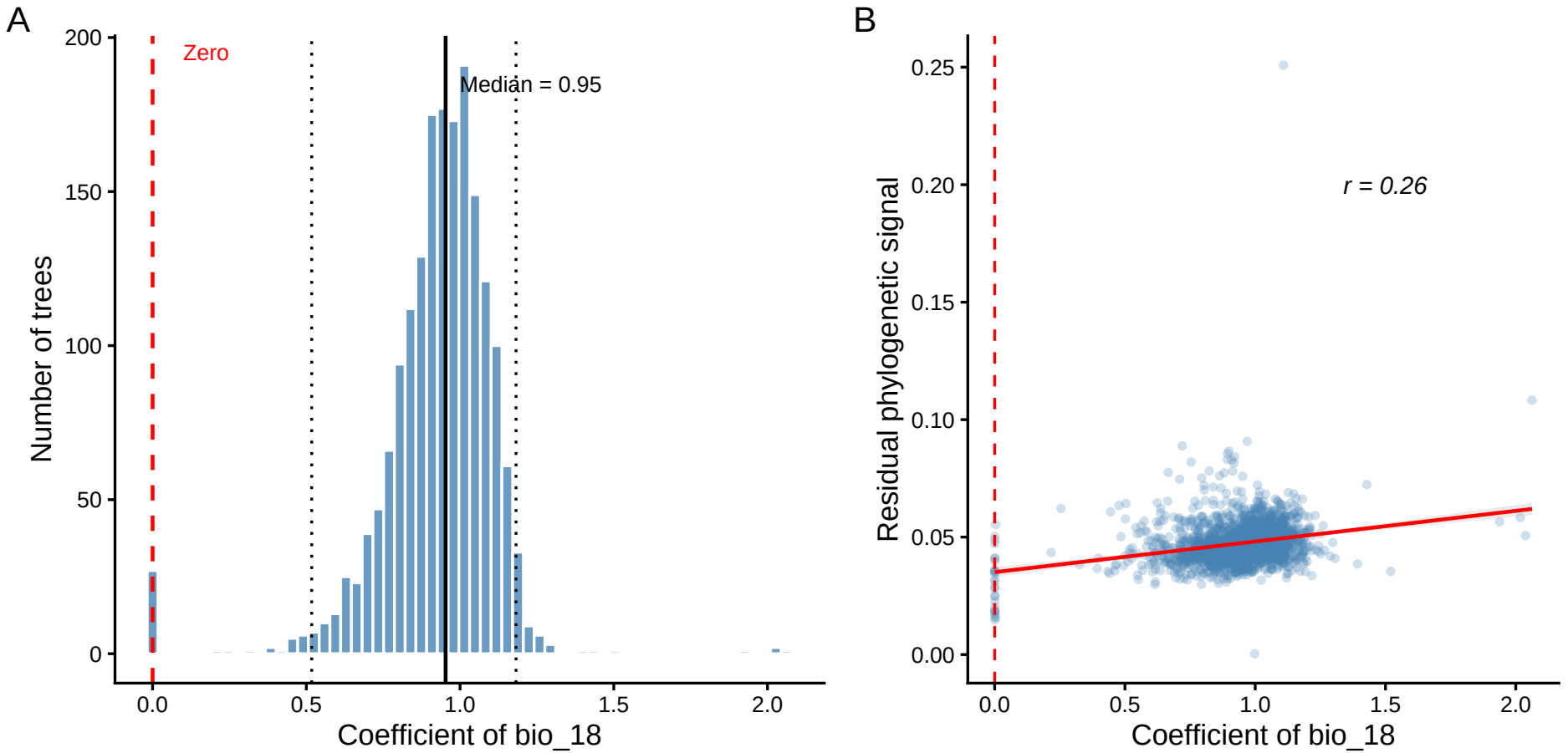
Figure S4. Sensitivity of the correlated-evolution test to alternative trait codings. Each of the 500 valid coding configurations (sampled from the 8192 possible combinations of fossoriality and diet states for the eight ambiguous taxa) was fitted under the independent and dependent models of correlated evolution in BayesTraits v4, and the resulting Bayes factor (BF = 2·ΔML) was computed for each configuration. (**A**) Distribution of BF across the 500 configurations. The solid red line marks the observed BF for the original coding (BF = 2.39); the dashed black line marks the median BF across configurations. The shaded area indicates configurations with BF greater than the observed value. (**B**) Empirical cumulative distribution of BF across configurations. The observed BF falls at the 18th percentile, indicating that approximately 82% of alternative codings yield a BF greater than the one obtained with the original coding. (**C**) Running mean of BF as configurations are added in their original order; the shaded band shows the running 95% confidence interval. The mean stabilizes well before the full set of configurations is reached, indicating that the estimate is not driven by a small subset of codings. (**D**) Detail of the distribution between BF = −2 and BF = 8, highlighting the position of the observed BF relative to the bulk of the distribution. Across all panels, the dependent model was favored over the independent model in 97.6% of the configurations (BF > 0).

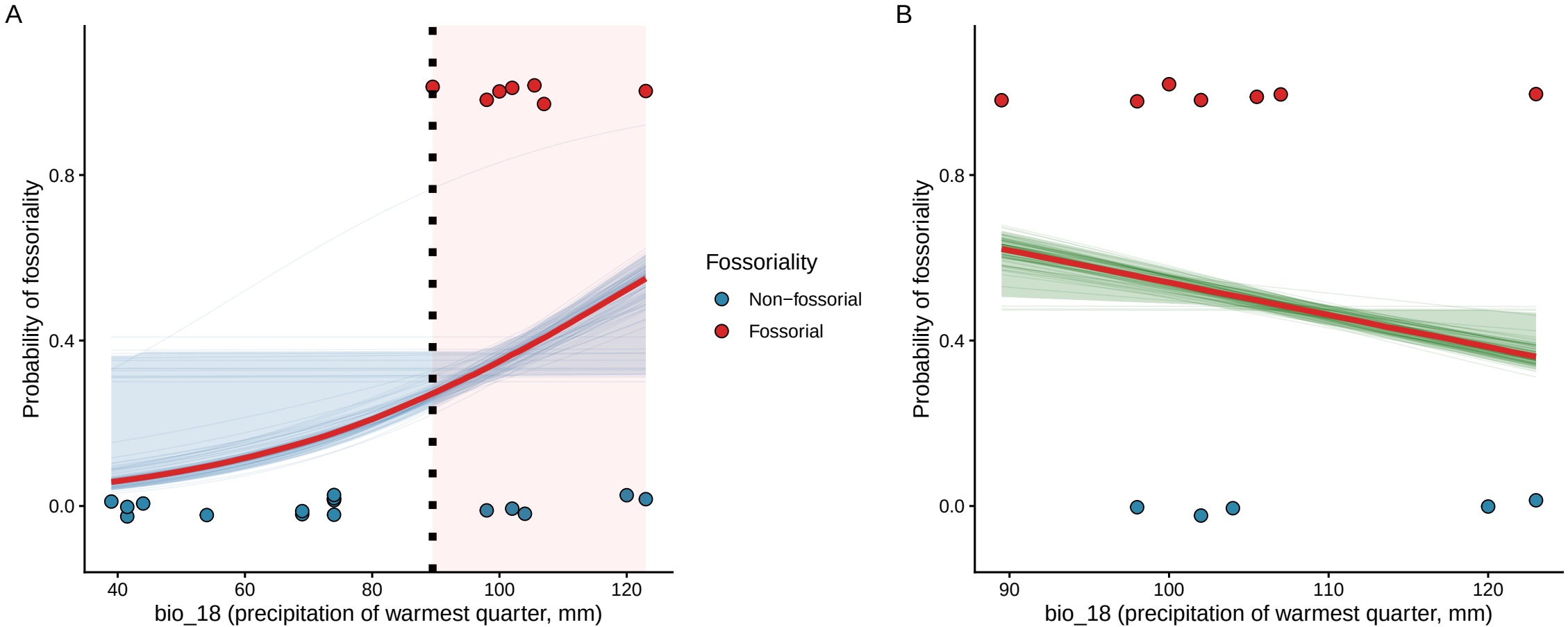
Table S1. Bioclimatic variables extracted from the Last Glacial Maximum (~21 ka) using the PaleoClim database at 5 arc-minutes resolution. All 19 variables were initially considered; six were retained after variance inflation factor (VIF) screening (see Table S2).

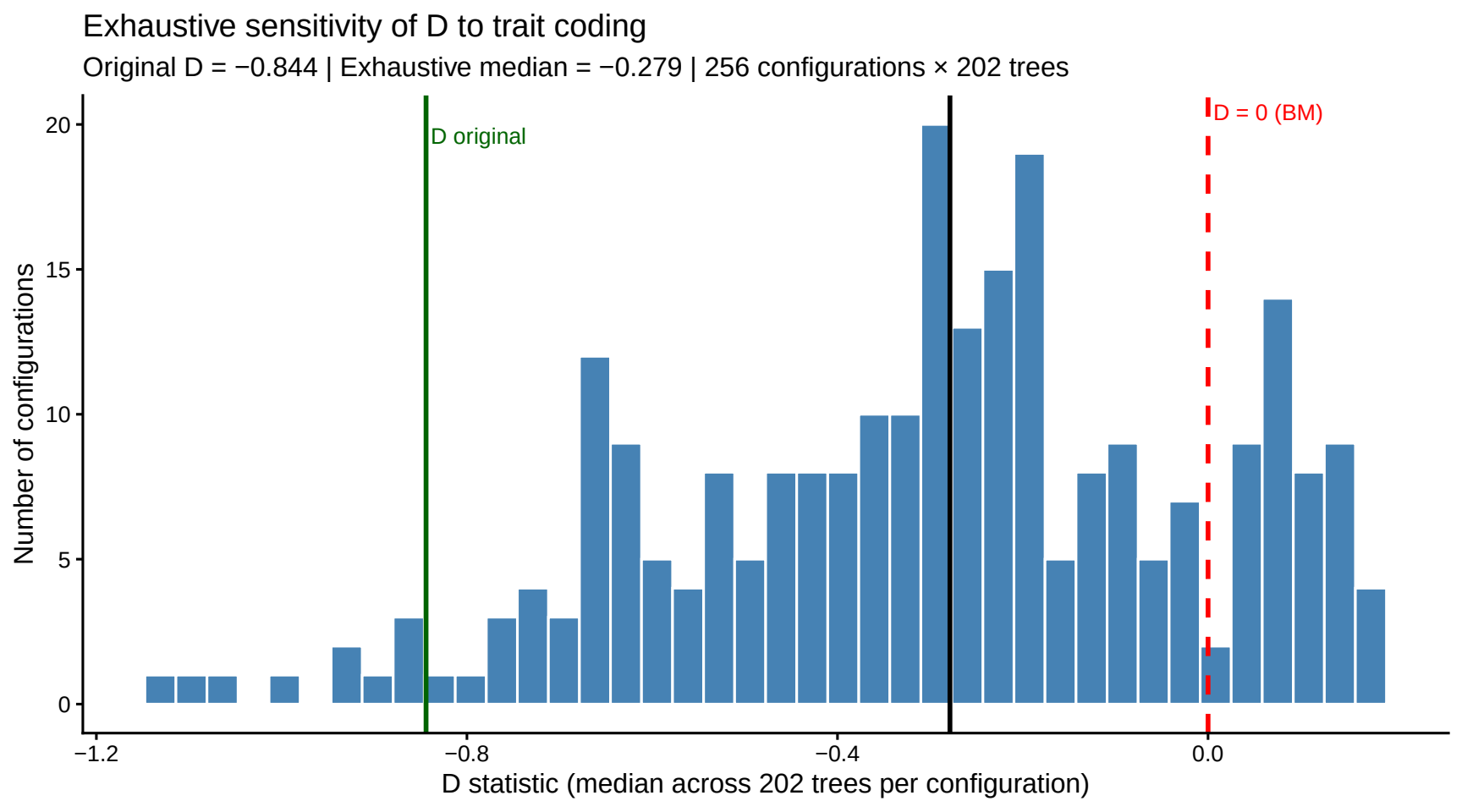
Table S2. Variance inflation factor (VIF) for the 19 bioclimatic variables, calculated on 10000 random points sampled across the geographic extent of the raster. VIF was computed on the available environmental space, independently of species occurrences, to avoid selection bias based on the realized niche. Variables with VIF > 3 were removed prior to downstream analyses.

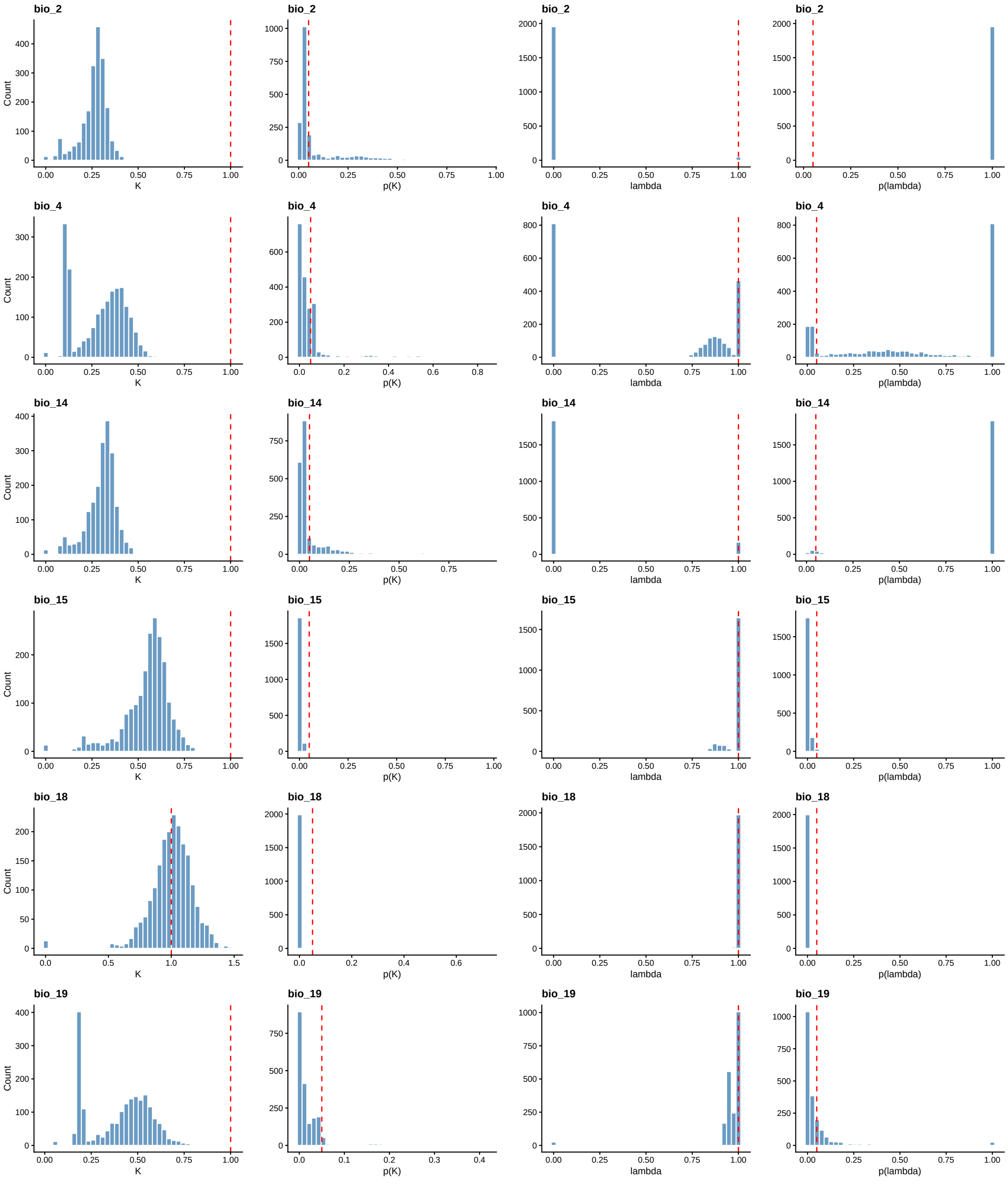

Dasypus novemcinctus
Glyptodon
Doedicurus sp
Cyclopes didactylus
Neocnus dousman
Parocnus serus
Neocnus comes
Acratocnus ye 2
Acratocnus ye 1
Nothrotheriops shastensis
Megatherium americanum
Megalonyx jeffersoni
Bradypus torquatus
Bradypus pygmaeus
Bradypus variegatus
Bradypus tridactylus
Scelidotherium
Scelidodon
Choloepus hoffmanni
Choloepus didactylus
Lestodon armatus
Paramylodon harlani
Mylodon darwinii
Glossotherium robustum
Non−fossorial
Fossorial

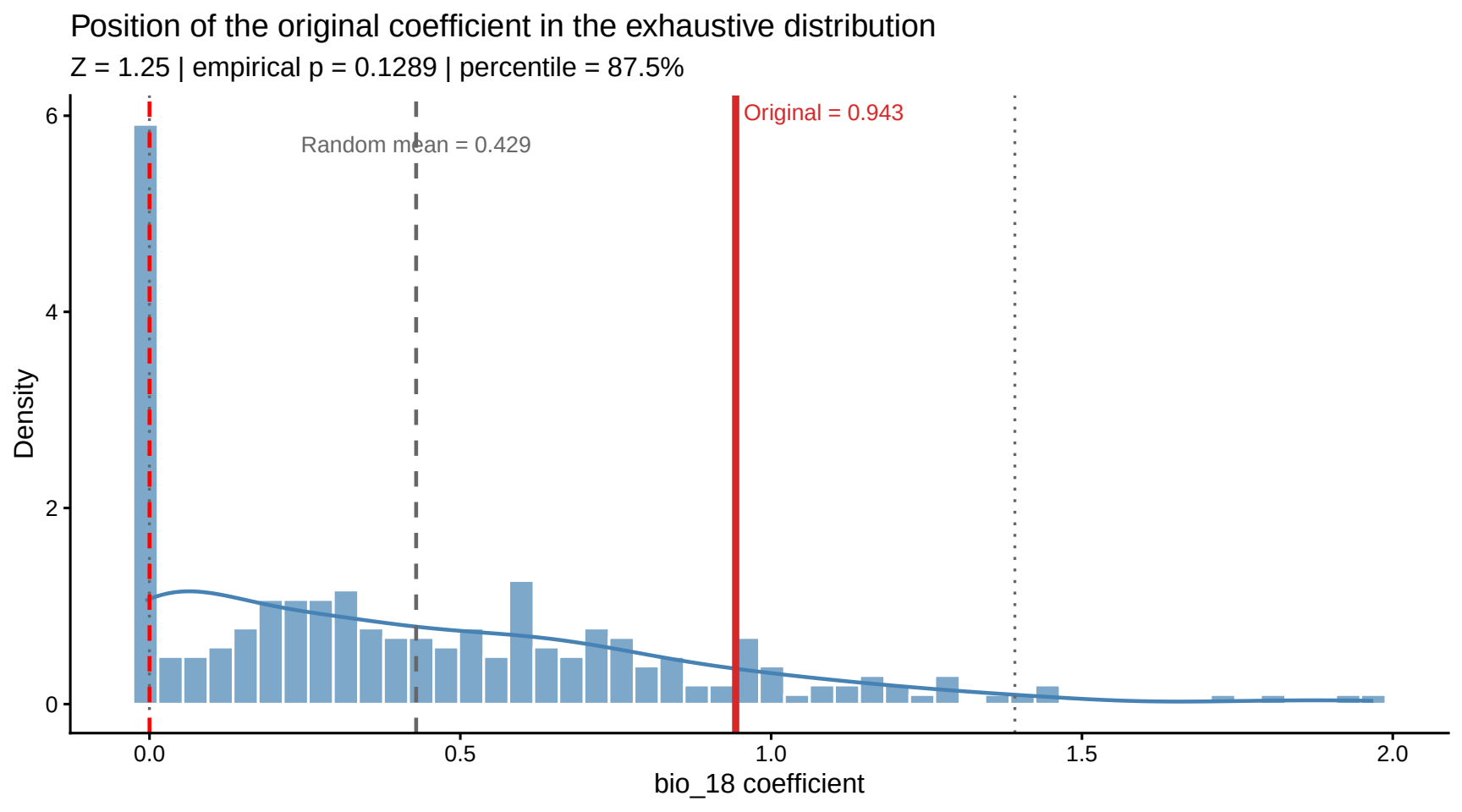

Median = −0.86
BM
Random
Number of Trees
200
150
100
50
0
−1
0
1
Fritz and Purvis' D statistic


A
Zero
Median = 0.95
Number of trees
200
150
100
50
0
0.0
0.5
1.0
1.5
2.0
Coefficient of bio_18
B
r = 0.26
Residual phylogenetic signal
0.25
0.20
0.15
0.10
0.05
0.00
0.0
0.5
1.0
1.5
2.0
Coefficient of bio_18


A
B
Probability of fossoriality
0.0
0.4
0.8
40
60
80
100
120
90
110
bio_18 (precipitation of warmest quarter, mm)
Fossoriality
Non−fossorial
Fossorial

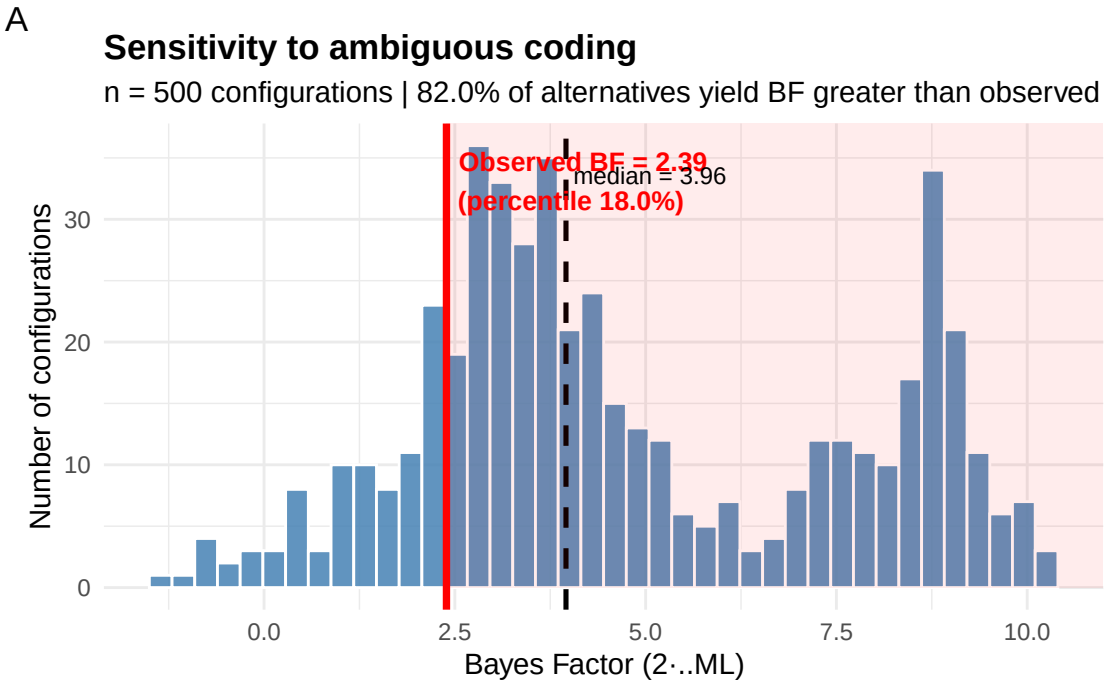

Exhaustive sensitivity of D to trait coding
Original D = −0.844 | Exhaustive median = −0.279 | 256 configurations × 202 trees
D original
D = 0 (BM)
Number of configurations
0
5
10
15
20
−1.2
−0.8
−0.4
0.0
D statistic (median across 202 trees per configuration)

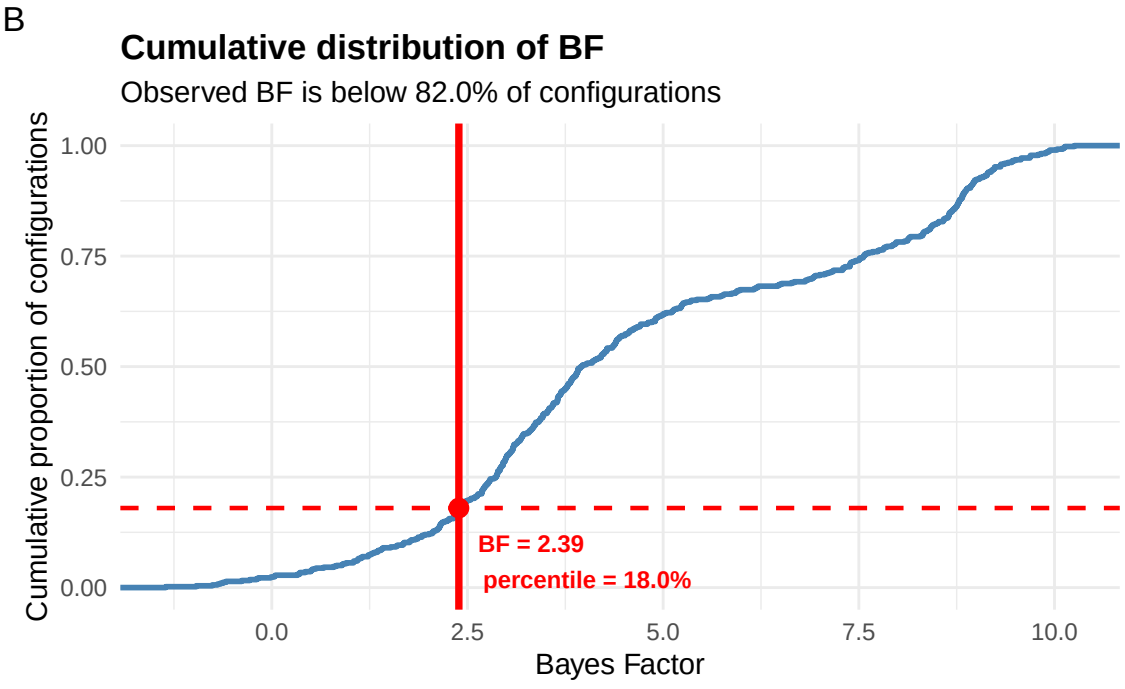

bio_2
bio_2
bio_2
bio_2
bio_4
bio_4
bio_4
bio_4
bio_14
bio_14
bio_14
bio_14
bio_15
bio_15
bio_15
bio_15
bio_18
bio_18
bio_18
bio_18
bio_19
bio_19
bio_19
bio_19
Count
K
p(K)
lambda
p(lambda)

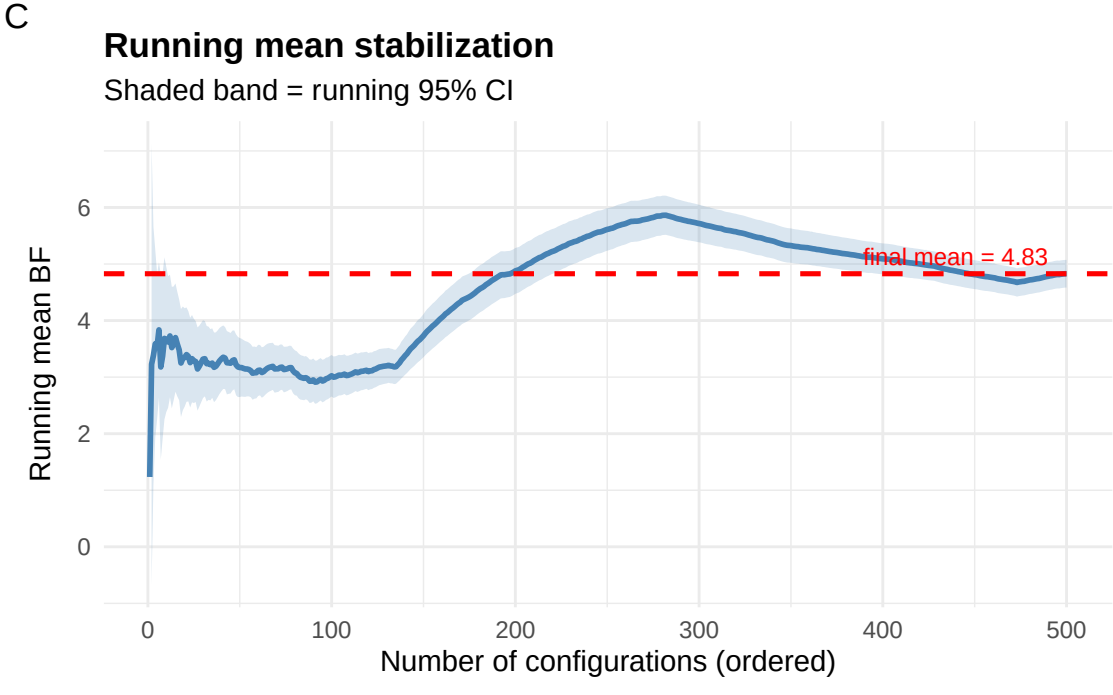

Position of the original coefficient in the exhaustive distribution
Z = 1.25 | empirical p = 0.1289 | percentile = 87.5%
Original = 0.943
Random mean = 0.429
Density
bio_18 coefficient
0
2
4
6
0.0
0.5
1.0
1.5
2.0

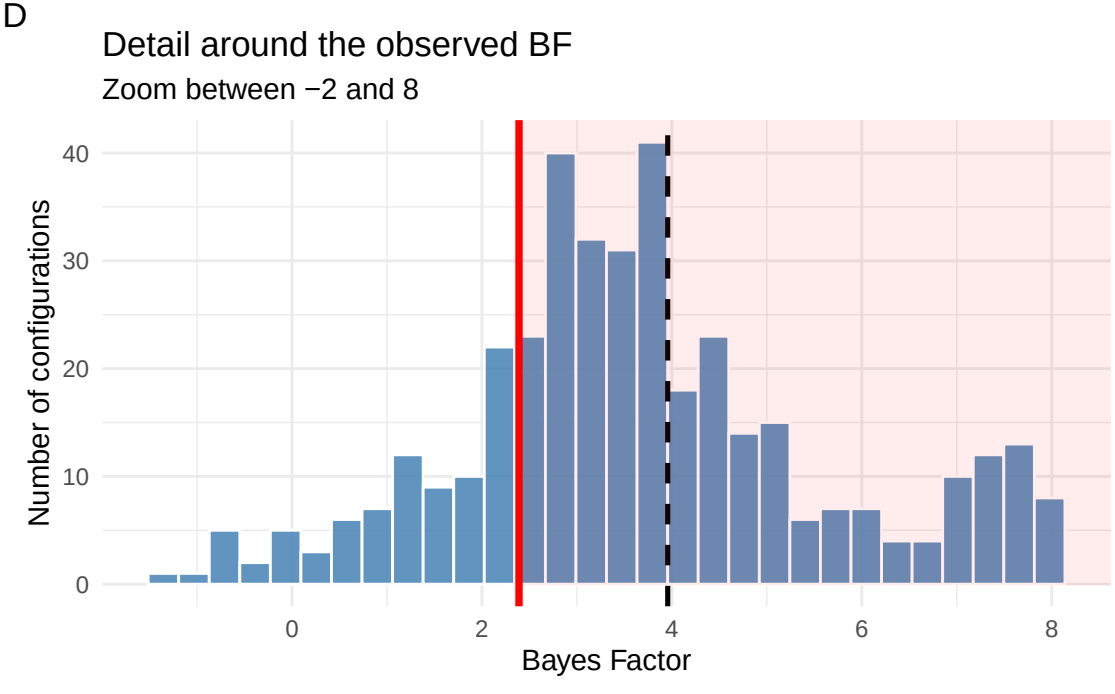
Sensitivity analysis to ambiguous coding

n = 500 configurations | observed BF = 2.39 (percentile 18.0%)









Variable	Bioclimatic variable	Status after VIF screening
BIO1	Annual Mean Temperature	Excluded
BIO2	Mean Diurnal Range	Retained
BIO3	Isothermality	Excluded
BIO4	Temperature Seasonality	Retained
BIO5	Max Temperature of Warmest Month	Excluded
BIO6	Min Temperature of Coldest Month	Excluded
BIO7	Temperature Annual Range	Excluded
BIO8	Mean Temperature of Wettest Quarter	Excluded
BIO9	Mean Temperature of Driest Quarter	Excluded
BIO10	Mean Temperature of Warmest Quarter	Excluded
BIO11	Mean Temperature of Coldest Quarter	Excluded
BIO12	Annual Precipitation	Excluded
BIO13	Precipitation of Wettest Month	Excluded
BIO14	Precipitation of Driest Month	Retained
BIO15	Precipitation Seasonality	Retained
BIO16	Precipitation of Wettest Quarter	Excluded
BIO17	Precipitation of Driest Quarter	Excluded
BIO18	Precipitation of Warmest Quarter	Retained
BIO19	Precipitation of Coldest Quarter	Retained

Variable	VIF
BIO2	1.192
BIO4	1.446
BIO14	2.858
BIO15	1.200
BIO18	1.745
BIO19	2.256